# Assembly of one-dimensional supramolecular objects: From monomers to networks

Mehmet Sayar*
*Department of Materials Science and Engineering, Northwestern University, Evanston, Illinois 60208, USA*

Samuel I. Stupp†
*Department of Materials Science and Engineering, Department of Chemistry, and Feinberg School of Medicine, Northwestern University, Evanston, Illinois 60208, USA*

(Received 15 July 2004; published 8 July 2005)

One-dimensional supramolecular aggregates can form networks at exceedingly low concentrations. Recent experiments in several laboratories, including our own, have demonstrated the formation of gels by these systems at concentrations well under 1% by weight. The systems of interest in our laboratory form either cylindrical nanofibers or ribbons as a result of strong noncovalent interactions among monomers. The stiffness and interaction energies among these thread-like objects can vary significantly depending on the chemical structure of the monomers used. We have used Monte Carlo simulations to study the structure of the threads and their ability to form networks through bundle formation. The persistence length of the threads was found to be strongly affected not only by stiffness, but also by the strength of attractive two-body interactions among thread segments. The relative values of stiffness and attractive two-body interaction strength determine if threads collapse or create bundles. Only in the presence of sufficiently long threads and bundle formation can these systems assemble into networks of high connectivity.

DOI: 10.1103/PhysRevE.72.011803 PACS number(s): 61.25.Hq, 82.35.−x, 05.65.+b

## I. INTRODUCTION

Gels made from synthetic and biological molecules are useful in a broad range of applications that include food technology, cosmetics, drug delivery, tissue engineering, cell transplantation, and many others [1–5]. Gels are typically networks formed by objects such as polymers, colloids, and small molecules known as gelators. In this paper we focus on networks formed by one-dimensional supramolecular structures. There is an extensive literature on such structures, which consist of polymers formed by noncovalent association among monomer molecules that do not necessarily form networks [6,7]. However, the thread-like objects of interest here have the capacity to form networks and most important, have a well defined cross section formed by the self-assembly of molecules. The cross sections can be either single molecules [4] or a specific assembly of several molecules [8–10]. The well defined cross section, which distinguishes them from ordinary polymers, offers properties such as extraordinary persistence length. One consequence of a long persistence length is the possibility of forming networks at extremely low concentration of molecules. Our laboratory reported recently on systems in which the cross section is formed by the assembly of peptide amphiphile molecules in water [8,9] or dendron rodcoil molecules in organic solvents [10].

The systems of interest here can be regarded as hierarchical structures with two different levels of organization, which are both driven by noncovalent bonds (i.e., hydrogen bonding, $\pi$-$\pi$ stacking, and metal-coordination bonds). The gelator molecules assemble to form the threads, and attractive two-body interactions provide the connectivity of the network. Since these systems involve only noncovalent bonds, they are reversible and highly sensitive to ionic strength, *p*H, temperature, concentration, and solvent. The interthread connectivity could either be in the form of defects (i.e., fusion of threads at a junction point), or via attractive short-range two-body interactions (such as bundling of threads through hydrogen bonding). The reversible hydrogel formed by self-assembling artificial proteins is an example in which the junctions are formed by bundling of $\alpha$-helices [11]. It is important to note that in networks formed by supramolecular threads, the critical concentrations for gel formation lie well below those associated with mesophase formation (i.e., liquid crystals) [12]. In fact gelation could be observed at concentrations as low as 1.0% [4,5,10,13]. As suggested before, this is a consequence of an extremely long persistence length of the thread-like objects [8–10,12,14].

Self-assembled networks have also been the subject of many recent theoretical studies [15–23]. The theory of thermoreversible gels formed by associating polymers is similar to the problem under consideration here. Even though it does not involve thread formation, it deals with the problem of network formation as a result of a finite number of bonding sites per chain [19–23]. On the other hand, end-linked polymers provide a special case, where the functionality per chain is limited to 2. One could obtain gels from end-linked polymers via multifunctional crosslinkers, and optimum values of the fraction of crosslinkers to thread ends have been previously studied such that defect-free network structures are formed [24]. An interesting case is offered by polymers in which a thermally driven conformational change leads to network formation [22]. This system is unique in the sense that the number of network junction sites is controlled by external effects. Good examples for such systems are natural

*Current address: Max Planck Institut für Polymerforschung, Mainz D-55128, Germany. Email address: sayar@mpip-mainz.mpg.de
†Corresponding author. Email address: s-stupp@northwestern.edu

 

and synthetic polypeptides, which can undergo helix-coil transitions.

Living polymers, where the polymerization of the monomers is reversible, also provides a closely related system to the problem under consideration [25–32]. Chain properties such as molecular weight distribution and radius of gyration, as a function of density and temperature, have been previously studied in the absence of attractive interactions among polymer chains [25]. Milchev *et al.* have studied living semiflexible polymers with attractive interactions using two- and three-dimensional grand canonical ensemble simulations [26]. These authors looked at the order-disorder transition and cluster-size distribution of living polymers, and concluded that in 3D systems, the phase transition is always first order and chain lengths follow an exponential probability distribution. Furthermore, Milchev *et al.* have also shown that molecular weight distribution in the dilute limit can be described by the Schultz-Zimm distribution and becomes purely exponential in the semidilute limit [33]. The gel transition for living polymers has been studied by Ballone and Jones in the presence of multifunctional active sites [32].

As mentioned above, an important feature of the supramolecular threads with a defined cross section is their extremely high persistence length. Bug *et al.* have studied the role of attractive two-body interactions on the percolation threshold for rod-like objects [17,18]. However, bundle formation was not taken into account in this work. Another important question is how the bundling of objects affects the critical concentration to create a network. In addition to polymers and low molar mass gelator molecules, networks have also been observed in ferromagnetic colloids, and theoretical work has been carried out to explain their formation [15,16].

In this work we study the formation of one-dimensional supramolecular threads from monomers, and the simultaneous formation of networks through attractive two-body interactions. We specifically study the role of attractive two-body interactions and thread stiffness on the structural properties of the threads and networks formed, whereas the temperature and concentration are kept constant in all simulations. Furthermore, we discuss the role of bundling and high persistence length on the connectivity of the network.

## II. MODEL

On- and off-lattice Monte Carlo simulations have been widely used for simulation of polymeric systems [34,35]. Off-lattice simulations provide a continuum representation of the threads, and therefore do not impose artificial limitations on bond lengths and bond angles. On the other hand lattice Monte Carlo simulations are computationally more attractive due to the discretized configurational space that enables the representation of the configuration of the system with integer numbers only. However, it is also well known that the lattice artifacts might significantly alter the simulation results in polymeric systems. Simple cubic lattice models of polymeric systems lead to configurations that are not possible to reach and not possible to relax, and also limit the bond angles to 0° and 90°, and the bond length to the lattice size [36,37]. The bond fluctuation method [37,38] (BFM) has been employed to overcome such problems, especially in simulations of dense polymeric systems. In 3D implementation of this model, eight lattice sites on a cubic lattice represent one monomer along the chain. Unlike the classical lattice simulations, BFM allows the bond length to fluctuate within a certain range. The range of allowed bond lengths is chosen such that excluded volume constraints are satisfied (i.e., no overlaps), and no bond intersections can take place during the Monte Carlo moves.

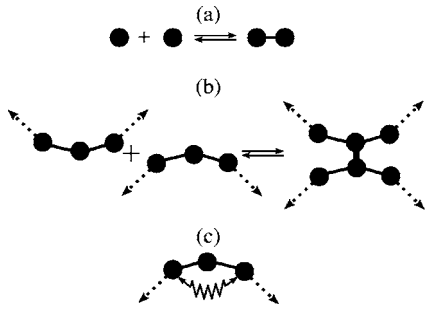


FIG. 1. Energy of the model includes contributions from bonds (a), attractive two-body interactions (b) (of strength $\epsilon$ and $\chi$, respectively), and thread stiffness (c) (of strength $\kappa$).

Here, we use a variation of BFM on hexagonal lattice. The model system is composed of individual gelator molecules represented by point particles on the lattice. Each gelator can make up to two bonds of energy $\epsilon$ [Fig. 1(a)], leading to linear thread formation. In addition to these bonds, each gelator has attractive two-body interactions of energy $\chi$ with gelators within the cutoff radius [Fig. 1(b)]. It is important to note that the bonding interactions are considered to be an order of magnitude stronger compared to two-body interactions. For each gelator $n_\epsilon$ represents the number of bonds and $n_\chi$ represents number of contacts formed by two-body interactions. The threads formed by polymerization of these gelators are semiflexible [Fig. 1(c)], where the stiffness is represented by a harmonic potential of strength $\kappa$. For any three gelators bonded along a thread, there is an energetic contribution of

$$E_\theta = \kappa(1 - \theta/\pi)^2, \tag{1}$$

where $\theta$ is the angle between the three gelators.

The simulations start with a random distribution of gelators on the hexagonal lattice with unit cell dimensions $a$. Initially the gelators have no bonds [Fig. 2(a)]. Each gelator has an excluded volume such that no two gelators can be closer than $4a$. If the distance $l$ between two gelators satisfies the condition $4a \leqslant l \leqslant 6a$, bonds can be formed. This specific choice of constraints guarantees the condition for no bond crossing during the simulation, and furthermore enables a wide range of values for bond length and angle. The cutoff radius for attractive two-body interaction is set equivalent to the maximum bond length ($6a$). In this study no energetic term is included for bond stretching. At each Monte Carlo step a target gelator is chosen at random, and a new position for this target gelator is randomly selected among the 12 nearest neighbor lattice points. If this new site does not vio-

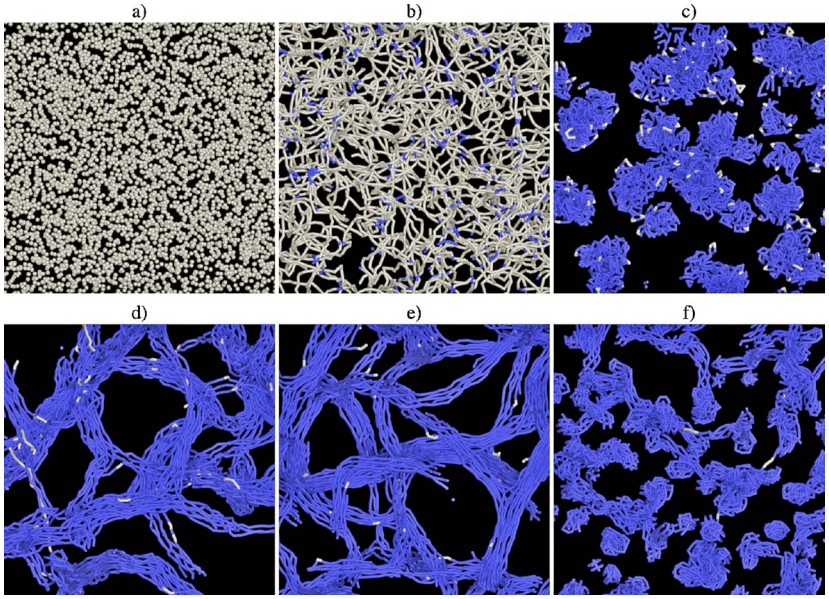


FIG. 2. (Color online) Snapshots from the simulation, where blue (dark) and white color represents the gelators with and without contacts formed by two-body attractive interactions, respectively. Only a representative part of the simulation box is shown. (a) Initial configuration of the system, randomly distributed nonbonded gelators. (b) For $\hat{\chi}=0.0$ and $\hat{\kappa}=6.28$, the gelators polymerize to form the dispersed threads. (c) For $\hat{\chi}=1.0$ and $\hat{\kappa}=1.57$, highly flexible threads form collapsed globules due to attractive two-body interactions. (d) For $\hat{\chi}=1.0$ and $\hat{\kappa}=6.28$, the stiffness of the threads prevents collapsing, and high persistence length threads with attractive two-body interactions form a connected network of bundles. (e) Further stiffening of the threads ($\hat{\chi}=1.0$ and $\hat{\kappa}=9.42$) provides higher order within the bundles. (f) Increasing the two-body attraction strength ($\hat{\chi}=3.0$ and $\hat{\kappa}=6.28$) causes the network structure to break into disconnected bundles of threads.

late any excluded volume constraints, the energies of the old and new configurations are calculated. In order to calculate the energy of the old configuration, the number of bonds $n_{\epsilon o}$ as well as any bending energy due to thread stiffness are taken into account. Furthermore, the attractive two-body interactions with gelators within the cutoff radius (where $n_{\chi o}$ is the number of these interactions) are included in the energy. This yields an energy of

$$E_{old} = -\epsilon n_{\epsilon o} - \chi n_{\chi o} + \sum_i \kappa(1-\theta_i/\pi)^2. \quad (2)$$

The bending energy term is only present if the target gelator is part of a thread with more than two gelators, and the index $i$ covers all bond angles the target gelator participates in. For the new configuration, first all the existing bonds of the target gelator are checked. If any of the old bonds are broken (i.e., the distance between two bonded gelators is larger than $6a$), or if any of the two bonding capacities are available ($n_{\epsilon o}<2$), a new bonding partner is searched. If there are any gelators with $n_{\epsilon}<2$ within the $6a$ cutoff radius, one ($n_{\epsilon o}=1$) or two ($n_{\epsilon o}=0$) gelators are chosen at random. Finally, the energy of this new configuration is obtained for $n_{\epsilon n}$ bonds and $n_{\chi n}$ two-body interactions, as

$$E_{new} = -\epsilon n_{\epsilon n} - \chi n_{\chi n} + \sum_i \kappa(1-\theta_i/\pi)^2. \quad (3)$$

Next, using the energy difference ($E_{new}-E_{old}$) the Boltzmann factor is calculated and the move is accepted or rejected according to the Metropolis algorithm. It is important to note that in this study we did not include a statistical factor for the formation and breaking of bonds other than the energetic contributions. The simulations are done on a hexagonal lattice with periodic boundary conditions and of size $400a$ in all three dimensions. For each set of molecular parameters, a system with 20 000 gelators, which corresponds to 2% volume fraction in a densely packed system, is used, and the results are obtained by taking an average over three different runs with different random seeds. In order to accelerate the simulation, the simulation box is divided into cells [34].

## III. RESULTS AND DISCUSSION

Our model includes three parameters to represent the molecular interactions in the experimental system. The parameter $\epsilon$ represents the strength of bonding along the threads and is kept constant as $\epsilon/k_BT=10.0$ for all simulations. For simplicity in the following sections rescaled values of $\hat{\chi}=\chi/k_BT$ and $\hat{\kappa}=\kappa/k_BT$ values will be used. In Figs. 2(b)–2(f), snapshots from simulations with different values of thread stiffness $\kappa$ and two-body interaction strength $\chi$ are given. For systems with no two-body attraction ($\hat{\chi}=0.0$ and $\hat{\kappa}=6.28$) the gelators simply form linear threads which are dispersed into the solution, just as one would observe in a polymerization reaction. The white colored thread monomers represent the gelators that have no two-body interactions, whereas the blue color represents the gelators that have at least one two-body interaction. In this case, two-body interactions are not stable against thermal fluctuations, and therefore the threads remain disconnected. A system with a moderate two-body attraction ($\hat{\chi}=1.0$) and highly flexible threads ($\hat{\kappa}=1.57$) yields a solution of collapsed globules [Fig. 2(c)]. During polymerization, threads simply collapse onto themselves due to attractive two-body interactions. Notice that there is no order within these collapsed structures. With the same two-body interaction strength ($\hat{\chi}=1.0, \hat{\kappa}=6.28$), if one increases the thread stiffness the structure of the aggregates completely changes [Fig. 2(d)]. Now the threads have a much higher persistence length and they do not form collapsed globules. Instead, by forming bundles they satisfy the two-body attractive forces, while avoiding the penalty of thread bending. The presence of long threads that participate in more than one bundle provides the connectivity among these ordered bundles; in other words, one observes a connected network of bundles. Further increase of the thread stiffness simply increases the order within these bundles

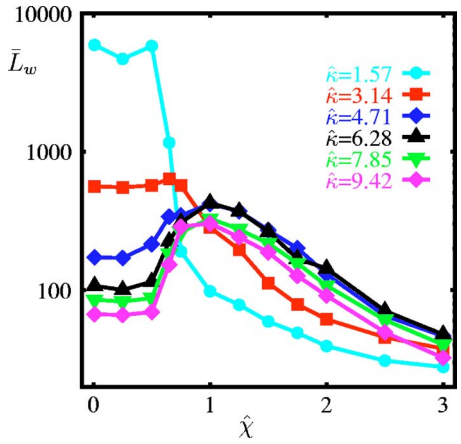


FIG. 3. (Color online) Weighted average thread length as a function of two-body interaction strength for different values of thread stiffness.

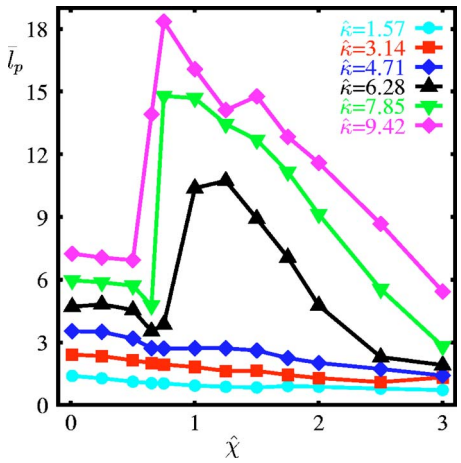


FIG. 4. (Color online) Persistence length of self-organized threads. Depending on the strength of the thread stiffness two different regimes are observed.

[Fig. 2(e)]. In the case of strong two-body interaction ($\hat{\chi}=3.0$) coupled with stiff threads ($\hat{\kappa}=9.42$), the system yields disconnected structures [Fig. 2(f)], but this time these substructures are highly ordered compared to the collapsed globules in Fig. 2(c).

It is important to note that these Monte Carlo simulations do not always guarantee thermodynamic equilibrium. In fact, some of the snapshots in Fig. 2 represent a kinetically trapped, glassy state. As the molecular threads form, the mobility of the gelators participating in the threads is highly reduced. Especially for the simulations with strong attractive two-body interactions and/or high stiffness values the acceptance ratio for the Monte Carlo moves is dramatically reduced. Even though initially the typical acceptance ratio for Monte Carlo moves is above 50%, in the final steady-state configuration the acceptance ratio drops to values as low as 5% for some simulation parameters. In this respect, our results are closely connected to the kinetic gelation model [39–45].

The Monte Carlo method utilized in this study is based on individual moves of the gelators. However, this leads to simulation artifacts that can be seen in the collapsed globular structures shown in Figs. 2(c) and 2(f). The globular structures in these snapshots have a reduced mobility. In thermodynamic equilibrium one would expect these globular structures to phase separate at low temperatures. However, due to the inefficiency of the single gelator Monte Carlo moves, these globular structures remain isolated in the simulation box, and macroscopic phase separation cannot be observed. These simulation artifacts can be overcome by introducing cluster moves into the algorithm. Such cluster moves could be designed to move the molecular threads, increasing the efficiency of the simulation algorithm. In this study, in order to keep the simulation of this complex system as simple as possible such cluster moves are not implemented. Furthermore, nonlocal moves (such as cluster moves) could lead to unphysical conformational changes, not suitable for studying glassy networks such as in Fig. 2(d).

In the remainder of this paper, we will look at the structural properties of this system to quantitatively understand the role of thread stiffness ($\kappa$) and attractive two-body interaction strength ($\chi$) on network formation. Since these simulations involve simultaneous polymerization and network formation, we need to analyze the structural properties of the threads (i.e., polydispersity, persistence length) and the clusters formed by such threads. In Fig. 3, the weighted averaged thread length $\bar{L}_w=\langle L_i^2\rangle/\langle L_i\rangle$ as a function of two-body interaction strength $\chi$ and thread stiffness $\kappa$ is shown. For the flexible threads ($\hat{\kappa}=1.57$) with weak two-body interactions $\hat{\chi}<0.5$ the length distribution is composed of a few extremely long threads and a lot of short segments. In fact, the polydispersity index in such systems can go as high as 50, which is in agreement with earlier predictions [33]. For flexible threads, polymerization also leads to cyclic structures and, together with the effect of attractive two-body interactions, this leads to collapsed globules [Fig. 2(c)], and inhibits thread growth. For simulations with $\hat{\kappa}>3.14$, three distinct regimes are observed. When the two-body interaction strength is weak compared to the thermal energy $\hat{\chi}<0.5$, the thread length is independent of $\chi$. In this linear regime, as the stiffness is increased above $\hat{\kappa}\geqslant 3.14$ the thread length decreases, since the loss of configurational entropy with increasing thread stiffness favors shorter thread lengths. On the other hand, when the two-body interaction is comparable to the thermal energy ($\hat{\chi}\approx 1.0$), a sharp increase in thread length is observed. The formation of bundles prevents collapse into globular structures, and since in a bundle a thread has already lost most of its configurational entropy, the enthalpic gain due to the growth of the chain is sufficient to increase the average thread length in the system. As for the third distinct regime, the sharp decline in the average thread length for $\hat{\chi}>1.0$ suggests that two-body interactions play a dominant role, thus leading to a collapsed structure.

The persistence length of the threads ($\bar{l}_p$) is another major factor in determining the final state of the network structure, and variation in $\bar{l}_p$ as a function of the two-body interaction strength and thread stiffness is shown in Fig. 4. The persistence length $\bar{l}_p$ of the threads is calculated from the exponential fit to the correlation function

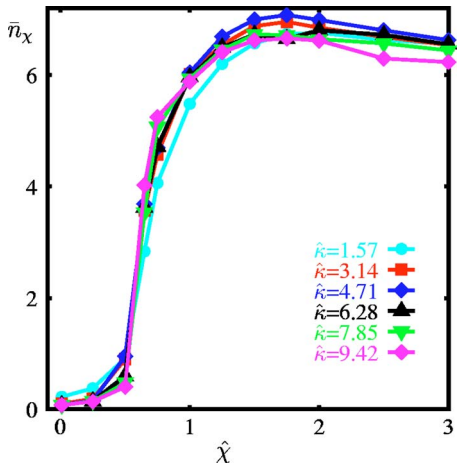


FIG. 5. (Color online) Average number of two-body interactions per gelator as a function of $\chi$ for different values of $\kappa$.

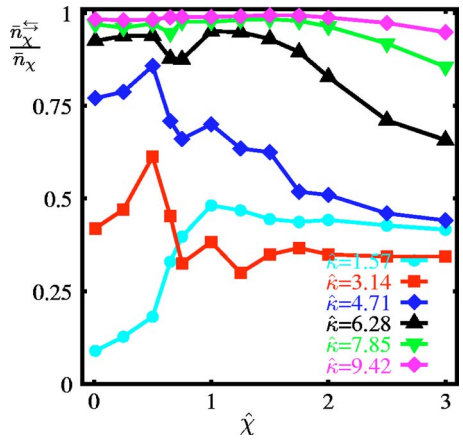


FIG. 6. (Color online) Fraction of two-body interactions among gelators of different threads to the total number of two-body interactions.

$$\langle \mathbf{u}(r) \cdot \mathbf{u}(0) \rangle = \exp(-r/\bar{l}_p), \tag{4}$$

where $\mathbf{u}(r)$ is the unit vector along the bond connecting gelator $r$ to gelator $r+1$. The sum is taken over all the threads in the system. With this definition $\bar{l}_p$ actually measures the persistence length in terms of the number of segments along the thread. The numerical data for the correlation length are cut off when a data point lies below zero, or $\langle \mathbf{u}(r) \cdot \mathbf{u}(0) \rangle$ is less than $\langle \mathbf{u}(r+1) \cdot \mathbf{u}(0) \rangle$. Two different parameter regimes are observed, depending on the thread stiffness. For simulations with $\hat{\kappa} \leqslant 4.71$, increasing $\hat{\chi}$ monotonically decreases the persistence length. In this regime the thread stiffness is soft enough that the equilibrium properties of the threads are mostly determined by the two-body interaction strength $\chi$. In other words, the aggregation state of the threads determines the persistence length. As we have seen in the snapshots from the simulation of flexible threads [Fig. 2(c)], during polymerization the threads simply collapse to form globules. On the other hand, for $\hat{\kappa} \geqslant 6.28$, a maximum in the thread persistence length is observed. This sharp increase in the persistence length is associated with the cooperative interplay of $\chi$ and $\kappa$, which favors aggregation of the threads into bundles. The bundling of these supramolecular threads lead to a higher persistence length, since within the bundles the threads are completely stretched, almost in a crystalline state. Over strengthening of $\chi$ destroys this balance and causes a sharp decrease of persistence length even for $\hat{\kappa} \geqslant 6.28$.

As explained above, this system exhibits two simultaneous phenomena; namely, polymerization and network formation. Besides the thread properties, we want to analyze the nature of the contacts among threads due to two-body interactions. In Fig. 5 the average number of two-body contacts ($\bar{n}_\chi$) per gelator is plotted as a function of $\chi$ and $\kappa$. Unlike our previous observations for thread properties, $\bar{n}_\chi$ is almost completely independent of the thread stiffness. At about $\hat{\chi} \approx 0.50$ we see a sudden jump in $\bar{n}_\chi$, and this value converges to $\approx 6-7$ contacts per gelator as $\chi$ is increased above the thermal energy. The saturation value of $\bar{n}_\chi$ is determined by the coordination number and the interaction cutoff radius.

As we have seen in the snapshots of the system in many cases the threads collapse into globular structures. Physical bonds formed by two-body interactions among gelators of the same thread lead to such collapsed structures. The percentage of such bonds also provides an insight into the thread conformation and therefore network connectivity. In Fig. 6 the ratio of contacts among gelators of different threads to the total number of contacts ($\bar{n}_\chi^{\leftrightarrows}/\bar{n}_\chi$) is plotted. For stiff threads ($\hat{\kappa} \geqslant 6.28$), most of the two-body interactions take place among gelators of different threads, and only for high two-body interaction strength ($\hat{\chi} > 2.5$), this fraction decreases below $\approx 90\%$. This is the regime wherein the majority of the threads are extended, and the threads are packed into bundles. As the stiffness of the threads is further lowered, the ratio $\bar{n}_\chi^{\leftrightarrows}/\bar{n}_\chi$ decreases. The simulations with $\hat{\kappa} = 1.57$ follow a quite different pattern compared with all other stiffness values, the ratio $\bar{n}_\chi^{\leftrightarrows}/\bar{n}_\chi$ increases and converges to 50% with increasing $\chi$. As explained before for $\hat{\kappa} = 1.57$, most of the threads polymerize to form very short cyclic structures. The increase in the $\bar{n}_\chi^{\leftrightarrows}/\bar{n}_\chi$ ratio is associated with the aggregation of these short thread segments.

Percolation theory has been widely used to study network formation in a variety of systems [46]. For a lattice model where the network forming elements are only one lattice point, one can define the gelation point as the divergence of the average connected aggregate size. However, for a system of chains in solution, one has to differentiate between phase separation and network formation [25]. In such a system, phase separation would also yield a connected structure, but this structure would not necessarily yield a spanning network. In our case, we not only have a dilute solution of threads, but in addition, the thread length is not constant. In many cases, the system size is not sufficiently big to measure a statistically valid gelation point. Therefore, rather than measuring the gelation point, we have used the following method to quantify the connectivity of the network.

In any given network, connectivity can be calculated by using an adjacency (connectivity) matrix [47]. Given a network of $N$ nodes one can form an $N$ by $N$ matrix such that the $ij$th element of this matrix is one if there is at least one

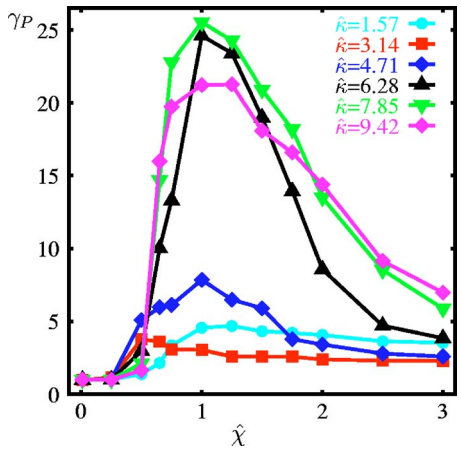


FIG. 7. (Color online) Primary connectivity value ($\gamma_P$) as a function of two-body interaction strength $\chi$ for different values of thread stiffness $\kappa$. $\gamma_P$ shows a maximum at $\chi \approx 1$, which suggests the influence of bundling on connectivity of the threads.

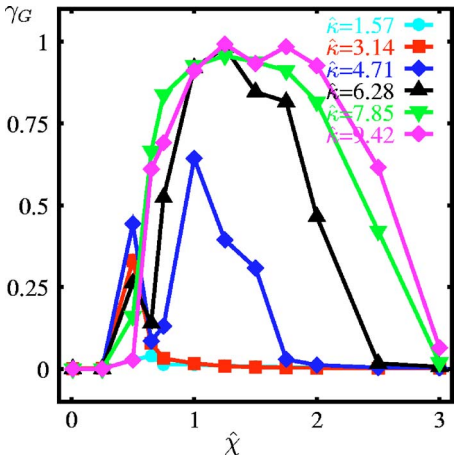


FIG. 8. (Color online) Global connectivity number as a function of two-body interaction strength $\chi$ for different values of thread stiffness $\kappa$. Increasing $\kappa$ extends the range of $\chi$ values that yield a highly connected network.

direct path from node $i$ to node $j$ or if $i=j$ [Eq. (5)]. Let us call this matrix as the primary connectivity matrix ($P$). Using this matrix one can obtain higher connectivity maps of this network, by simply raising $P$ to higher powers. For example, $P^2$ provides a new matrix, where the elements show the number of different paths between any two nodes by taking up to two steps. $P^{(N-1)}$ yields the global connectivity matrix ($G$), where the elements of $G$ are nonzero if there is at least one path that connects node $i$ to node $j$ [Eq. (6)]:

$$P_{ij} = \begin{cases} 1, & i = j, \\ 1, & \text{threads } i \text{ and } j \text{ directly connected}, \\ 0, & \text{otherwise}, \end{cases} \tag{5}$$

$$G_{ij} = \begin{cases} \neq 0, & \text{path } i \to j \text{ exists}, \\ 0, & \text{otherwise}. \end{cases} \tag{6}$$

Since we are interested in the connectivity of the threads, we will work in the dual space. In the dual space representation, each thread will be considered as a node (vertex) and physical bonds that connect threads to each other will be considered as paths (edges). A system composed of $N$ threads can then be mapped on to a network of $N$ nodes, where two-body interactions form the connecting paths among the threads (nodes). Whether two threads are connected at a single point or they touch at more than one point (entangled) does not change the contribution of these threads to the global connectivity. For any given snapshot of the system, in our analysis two threads are considered to have a stable contact only if the total energy of the two-body interactions among them is $\geqslant 3k_BT$. Thermal fluctuations lead to formation of many contacts during the simulation. If the two-body interaction strength is strong enough and the neighboring gelators along the threads are reoriented, this leads to a sequence of two-body interactions along the threads. In this case, even if some of these contacts break, the surrounding contacts prevent rapid diffusion of gelators, and therefore increase the chances for reformation of the broken contact. Only such stable contacts lead to the formation of structures as we have seen in Figs. 2(c)–2(f). On the other hand, contacts formed in a system with weak two-body interactions [Fig. 2(b)], only last for a few simulation steps and are considered to be unstable in terms of the structural integrity of the network. $P$ and $G$ can be used to quantify the degree of connectivity in any given network. One can define a primary connectivity number ($\gamma_P$) as

$$\gamma_P = \left( \sum_{ij} P_{ij} \right) / N - 1 \tag{7}$$

(−1 is for excluding the self connectivity), and a global connectivity number ($\gamma_G$) as

$$\gamma_G = \left( \sum_{i<j} G_{ij} \right) / [N(N-1)/2]. \tag{8}$$

The value of $\gamma_P$ is calculated from a snapshot of the equilibrated system for any given set of molecular parameters. $\gamma_P$ yields the average number of physical contacts per thread. For all values of thread stiffness $\kappa$, the $\gamma_P$ curves have a maximum around $\hat{\chi} \approx 1.0$ (Fig. 7). The maximum primary connectivity values highly depend on the thread stiffness $\kappa$, increasing with increasing thread stiffness and saturating as one reaches high $\kappa$ values. For $\hat{\chi} < 0.5$ the thermal energy does not allow any stable connections; therefore, the system is composed of disconnected threads. The maximum observed around $\hat{\chi} \approx 1.0$ is an indication of stable two-body interactions. As we have explained above, the formation of bundles enhances organization of the threads and therefore we observe an increased $\gamma_P$. Upon further increase of the two-body interaction strength, this fine balance is destroyed and the $\gamma_P$ value declines sharply.

The global connectivity ($\gamma_G$) values (Fig. 8) provide a quantitative value for the overall connectivity in the equilibrated system. Unlike the previous analysis, where the results were averaged over all threads, the $\gamma_G$ values represent only an average over the final state of three different runs for each given parameter set. The global connectivity $\gamma_G$ can

vary between 0 and 1. $\gamma_G=0$ represents the case in which all threads in the system are isolated and do not have any stable contacts with any of the neighboring threads. On the other hand, $\gamma_G=1$ represents a system wherein all the threads are part of a single network. In other words, for $\gamma_G=1$ there exists at least one path between any two threads in the system. Except for $\hat{\kappa}=1.57$, for all $\kappa$ values we observe a maximum in the global network connectivity. The range of two-body interaction values that yield a highly connected network increases with the stiffness of the threads. As observed in the snapshots, for extremely low or high $\chi$ values a connected network does not exist. The drop in the global connectivity for $\hat{\kappa} \leqslant 4.71$ is not well understood and is currently being investigated. For low $\chi$, thermal energy does not allow any stable two-body interactions, and for very high $\chi$ the threads collapse to form globular disconnected structures. Only at optimum values of $\chi$ and $\kappa$ is a highly connected network structure observed.

## IV. CONCLUSIONS

We have used Monte Carlo simulations to study the assembly of supramolecular threads into networks. The persistence length of the threads was found to be strongly affected not only by stiffness but also by the strength of interactions among thread segments. The relative values of stiffness and interaction strength determine if threads collapse or create bundles. Only in the presence of sufficiently long threads and bundle formation can these systems assemble into networks of high connectivity.

## ACKNOWLEDGMENTS

This work was supported primarily by the Nanoscale Science and Engineering Initiative of the National Science Foundation under NSEC Grant Number EEC-0118025. We would also like to acknowledge support from DOE Grant Number DE-FG02-00ER-54810.

[1] M. Djabourov, Polym. Int. **25**, 135 (1991).
[2] K. Y. Lee and D. J. Mooney, Chem. Rev. (Washington, D.C.) **101**, 1869 (2001).
[3] K. H. Bouhadir, E. Alsberg, and D. J. Mooney, Biomaterials **22**, 2625 (2001).
[4] P. Terech and R. G. Weiss, Chem. Rev. (Washington, D.C.) **97**, 3133 (1997).
[5] D. J. Abdallah and R. G. Weiss, Adv. Mater. (Weinheim, Ger.) **12**, 1237 (2000).
[6] J. M. Lehn, *Supramolecular Chemistry* (VCH, New York, 1995).
[7] L. Brunsveld, B. J. B. Folmer, E. W. Meijer, and R. P. Sijbesma, Chem. Rev. (Washington, D.C.) **101**, 4071 (2001).
[8] J. D. Hartgerink, E. Beniash, and S. I. Stupp, Science **294**, 1684 (2001).
[9] J. D. Hartgerink, E. R. Zubarev, and S. I. Stupp, Curr. Opin. Solid State Mater. Sci. **5**, 355 (2001).
[10] E. R. Zubarev, M. U. Pralle, E. D. Sone, and S. I. Stupp, J. Am. Chem. Soc. **123**, 4105 (2001).
[11] W. A. Petka, J. L. Harden, K. P. McGrath, D. Wirtz, and D. A. Tirrell, Science **281**, 389 (1998).
[12] U. Beginn, G. Zipp, and M. Moller, J. Polym. Sci., Part A: Polym. Chem. **38**, 631 (2000).
[13] C. Geiger, M. Stanescu, L. H. Chen, and D. G. Whitten, Langmuir **15**, 2241 (1999).
[14] M. Sinclair, K. C. Lim, and A. J. Heeger, Phys. Rev. Lett. **51**, 1768 (1983).
[15] T. Tlusty and S. A. Safran, Science **290**, 1328 (2000).
[16] J. T. Kindt, J. Phys. Chem. B **106**, 8223 (2002).
[17] A. L. R. Bug, S. A. Safran, G. S. Grest, and I. Webman, Phys. Rev. Lett. **55**, 1896 (1985).
[18] A. L. R. Bug, S. A. Safran, and I. Webman, Phys. Rev. B **33**, 4716 (1986).
[19] A. N. Semenov, J. F. Joanny, and A. R. Khokhlov, Macromolecules **28**, 1066 (1995).
[20] F. Tanaka, Physica A **257**, 245 (1998).
[21] S. K. Kumar and A. Z. Panagiotopoulos, Phys. Rev. Lett. **82**, 5060 (1999).
[22] F. Tanaka, Macromolecules **33**, 4249 (2000).
[23] F. Tanaka, Polym. J. (Tokyo, Jpn.) **34**, 479 (2002).
[24] N. Gilra, C. Cohen, and A. Z. Panagiotopoulos, J. Chem. Phys. **112**, 6910 (2000).
[25] Y. Rouault and A. Milchev, Phys. Rev. E **51**, 5905 (1995).
[26] A. Milchev and D. P. Landau, Phys. Rev. E **52**, 6431 (1995).
[27] J. Dudowicz, K. F. Freed, and J. F. Douglas, J. Chem. Phys. **111**, 7116 (1999).
[28] J. Dudowicz, K. F. Freed, and J. F. Douglas, J. Chem. Phys. **112**, 1002 (2000).
[29] P. G. Khalatur, A. R. Khokhlov, J. N. Kovalenko, and D. A. Mologin, J. Chem. Phys. **110**, 6039 (1999).
[30] P. Ballone and R. Jones, J. Chem. Phys. **115**, 3895 (2001).
[31] P. Ballone and R. Jones, J. Chem. Phys. **116**, 7724 (2002).
[32] P. Ballone and R. Jones, J. Chem. Phys. **117**, 6841 (2002).
[33] A. Milchev, J. P. Wittmer, and D. P. Landau, Phys. Rev. E **61**, 2959 (2000).
[34] M. Allen and D. Tildesley, *Computer Simulation of Liquids* (Clarendon, Oxford, 1987).
[35] D. Frenkel and B. Smit, *Understanding Molecular Simulation* (Academic, New York, 2002).
[36] N. Madras and A. D. Sokal, J. Stat. Phys. **47**, 573 (1987).
[37] I. Carmesin and K. Kremer, Macromolecules **21**, 2819 (1988).
[38] H. P. Deutsch and K. Binder, J. Chem. Phys. **94**, 2294 (1991).
[39] *Numerical Methods in the Study of Critical Phenomena*, edited by I. Della, J. Demongeot, and B. Lacolle (Springer, New York, 1981).
[40] F. Family, Phys. Rev. Lett. **51**, 2112 (1983).
[41] P. Meakin, Phys. Rev. Lett. **51**, 1119 (1983).
[42] J. C. Gimel, D. Durand, and T. Nicolai, Phys. Rev. B **51**, 11348 (1995).
[43] H. J. Herrmann, D. P. Landau, and D. Stauffer, Phys. Rev. Lett. **49**, 412 (1982).
[44] J. M. Jin, K. Parbhakar, L. H. Dao, and K. H. Lee, Phys. Rev. E **54**, 997 (1996).
[45] T. Terao and T. Nakayama, Phys. Rev. E **58**, 3490 (1998).
[46] P. G. de Gennes, *Scaling Concepts in Polymer Physics* (Cornell University Press, Ithaca, 1996).
[47] T. H. Cormen, C. E. Leiserson, and R. L. Rivest, *Introduction to Algorithms* (MIT Press, Cambridge, MA, 2000).